Ethene Homopolymerization and Copolymerization with 1-Hexene for All Methyl-Substituted $(R_nC_5H_{5-n})_2ZrCl_2$/MAO Catalytic Systems: Effects of Split Methyl Substitution

HANNE WIGUM,[1] LINDA TANGEN,[1] JON ANDREAS STØVNENG,[1] ERLING RYTTER[1,2]

[1]Department of Chemical Engineering, Norwegian University of Science and Technology, N-7491 Trondheim, Norway

[2]Statoil Research Centre, N-7005 Trondheim, Norway

Received 21 April 2000; accepted 20 June 2000

ABSTRACT: Ethene homopolymerization and copolymerization with 1-hexene were catalyzed by methyl-substituted cyclopentadienyl (Cp) zirconium dichlorides, $(R_nC_5H_{5-n})_2ZrCl_2$ (R_n = H, Me, 1,2-Me_2, 1,3-Me_2, 1,2,3-Me_3, 1,2,4-Me_3, Me_4, or Me_5), and methylaluminoxane. The polymers were characterized with Fourier transform infrared, nuclear magnetic resonance, gel permeation chromatography, and differential scanning calorimetry techniques. Generally, an increasing number of methyl substituents on the Cp ligand results in lower 1-hexene incorporation in the copolymer. The two catalysts with split methyl substitution (R_n = 1,3-Me_2 and R_n = 1,2,4-Me_3) show a higher comonomer response than their disubstituted and trisubstituted counterparts (R_n = 1,2-Me_2 and R_n = 1,2,3-Me_3). They even incorporate more 1-hexene than R_n = H and R_n = Me. These findings are qualitatively in agreement with the results of a theoretical study based on density functional calculations. The presence of comonomer does not influence the termination reactions after the insertion of ethene. There is more frequent termination after each hexene insertion with increasing comonomer incorporation except for the two catalysts with split methyl substituents. The termination probability per inserted comonomer is highest for the less substituted catalysts. © 2000 John Wiley & Sons, Inc. J Polym Sci A: Polym Chem 38: 3161–3172, 2000

Keywords: copolymerization; zirconocene catalyst; methyl-substituted catalyst; density functional theory; comonomer response; ethene; 1-hexene; chain termination; Fourier transform infrared (FTIR); nuclear magnetic resonance (NMR); gel permeation chromatography (GPC); differential scanning calorimetry (DSC); successive self-nucleation/annealing (SSA)

INTRODUCTION

Metallocene catalysis of olefins is well known for its excellent ability to produce polymers with high molecular weight and narrow molecular weight distribution. The possibility of controlling the comonomer incorporation represents one of the key features. Through the copolymerization of ethene with another α-olefin, one obtains a linear polyethene with short chain branches and, consequently, low crystallinity and density.[1] Several studies show that for methylaluminoxane (MAO)-activated zirconocenes, the rate of copolymerization of ethene with α-olefins often exceeds that of ethene homopolymerization.[1–4] Olefin copolymer-

Correspondence to: E. Rytter (E-mail: erling.rytter@statoil.com)

Journal of Polymer Science: Part A: Polymer Chemistry, Vol. 38, 3161–3172 (2000)

ization behavior depends on the structure of the metallocene catalyst.[5,6] In general, syndiospecific (C_s symmetric) metallocene catalysts are more effective in incorporating α-olefins into an ethene copolymer than isospecific (C_2 symmetric) or unbridged ones.[7] The effect of ligands and their substitution pattern is a combination of electronic and steric effects and has been the objective of several studies. Möhring and Coville[8] studied different alkyl-substituted Cp ligands of Cp_2ZrCl_2/EAO catalysts and their influence on the copolymerization with C_5–C_{14} α-olefins. They reported that the copolymerization activity decreases with increasing steric bulk of the catalyst. Benzannelation of silylene-bridged bis(indenyl)zirconocene ligands increases comonomer incorporation, whereas 2-methyl substitution gives increased molar masses and reduced ethene copolymerization activity.[9,10] Hydrogenation of the indenyl ligands in different ansa metallocene complexes reduces the comonomer content and the molar masses of the ethene/1-hexene copolymers.[11] The ligand structure also influences the termination mechanisms and, consequently, the end groups of the polymers.[12,13] The ratio between vinyl and *trans*-vinylene unsaturation is approximately 6/1 with Cp_2ZrCl_2 and 1/1 with $Cp^*_2ZrCl_2$.[12] The objective of this work is to investigate the homopolymerization of ethene and the copolymerization of ethene and 1-hexene with zirconocene catalysts containing different methyl-substituted cyclopentadienyl (Cp) ligands. The influence of the number of methyl substituents and their positions is studied. The catalysts used are activated with MAO and have the general form $(R_nC_5H_{5-n})_2ZrCl_2$ (R_n = H, Me, 1,2-Me_2, 1,3-Me_2, 1,2,3-Me_3, 1,2,4-Me_3, Me_4, or Me_5). In Scheme 1, molecular models are shown for these eight catalysts. Optimized with density functional theory,[14–17] cations with an agostic interaction between Zr and γ-hydrogen on the growing polymer chain have been chosen as models for the active site.

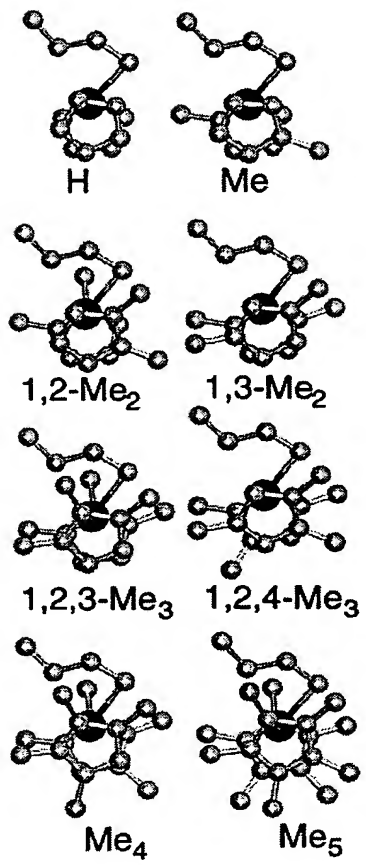

Scheme 1. Molecular structures of eight zirconocenes used in ethene homopolymerization and copolymerization with 1-hexene. The cations $(R_nC_5H_{5-n})_2ZrC_4H_9^+$ with an agostic interaction between Zr and a γ-hydrogen on the growing polymer chain serve as models for the active site (Zr, black ball; C, gray balls; H, omitted for clarity). Geometries were optimized with density functional calculations. Different conformations can be obtained by the rotation of the methyl-substituted Cp ligands around the Zr–Cp axes. The figure shows the lowest energy conformation for each catalyst. In general, energy differences, as well as energy barriers between the various conformations, increase with the addition of methyl substituents. For R_n = Me, nine conformations lie within a range of 1 kcal/mol, whereas for R_n = Me_4, all other conformations are more than 1 kcal/mol less stable than the one shown.

EXPERIMENTAL

Chemicals

Bis-cyclopentadienyl zirconium dichloride derivatives [$(R_nC_5H_{5-n})_2ZrCl_2$; Boulder Scientific Co.], 10 wt % MAO (4.67 wt % Al) in toluene (Albemarle S. A.), N_2 (Hydrogas), and ethene and 1-hexene (Borealis) were all used as received. Toluene (Merck) was refluxed for 3 h with sodium and distilled under a nitrogen atmosphere prior to use. Standard Schlenk techniques were used during all manipulations.

Polymerization

The catalysts were dissolved in toluene (100 mL). The steel autoclave was repeatedly flushed and evacuated both with nitrogen and ethene several times before toluene (200 mL) was introduced. For the copolymerizations, 1-hexene (10 mL) was then added to the reactor. The temperature was set to 80 °C, and the stirring rate was set to 2000 rpm. Ethene was introduced and equilibrated at 2 bar before the MAO solution was added 15 min prior to catalyst addition. The Al/Zr mole ratio was 3000 for all polymerizations, and the amount of catalyst was 0.12 or 0.24 μmol. The ethene pressure was held constant during the reaction, and the instantaneous consumption was measured. The reaction was stopped after 1 h by the closure of the monomer feed, and the product was immediately poured into a mixture of methanol (300 mL) and hydrochloric acid (30 mL) and stirred overnight. The product was then filtered and washed with methanol and dried in open air. In the copolymerizations, less than 10% of the added 1-hexene was consumed, except for run 24, where about 30% of the 1-hexene was consumed.

Polymer Characterization

For Fourier transform infrared spectroscopy (FTIR), the spectra were recorded on a Bruker IFS66V spectrophotometer equipped with a deuterated triglycine sulfate (DTGS) detector. Homopolymers and copolymers were pressed into discs approximately 500 μm thick, and 200 scans were taken. The difference between the spectra before and after bromination was used to measure the absorbance of the unsaturated end groups. Vinyl, *trans*-vinylene, and vinylidene contents were estimated from peak intensities at 908, 964, and 888 cm^{-1}, respectively, with corresponding molar extinction coefficients of 110, 168, and 146 $L \cdot mol \cdot cm^{-1}$. A modified literature expression[18] was employed to correct for the comonomer content to obtain unsaturations per 1000 C in the backbone of the polymer chain:

$$N_v = \frac{14 \cdot A_v \cdot (2x_H + 1)}{\rho \cdot l \cdot \varepsilon}$$

Here, N_v is the number of double bonds per 1000 C atoms in the backbone for a given end group (v), A_v is the absorbance, x_H is the molar fraction of hexene in the polymer, ρ is the polymer density, l is the disc thickness, and ε is the molar extinction coefficient. Polymer densities were estimated to range from 0.90 to 0.94 g/mL with literature values[19] and under the assumption that there is a linear relationship between ρ and the amount of 1-hexene incorporated. In the expression for N_v, the absorbance A_v is usually the least accurate figure, with an uncertainty of 5–10% but occasionally up to 30% for weak or partially overlapping bands.

Gel permeation chromatography (GPC) was performed with a Polymer Laboratories PL-210 GPC instrument equipped with two PL gel 10-μm mixed-B columns and was operated at a flow rate of 1.0 mL/min and a temperature of 160 °C in the oven. Procedures were performed as previously described.[20]

Differential scanning calorimetry (DSC) was performed according to previously reported procedures.[21] The fractionation method based on successive self-nucleation/annealing (SSA) was performed with DSC.[22] The polymer was first melted at 170 °C and subsequently cooled to 25 °C (10 °C/min). The samples were then successively heated to a selected self-seeding and annealing temperature, T_s, where it was kept for 5 min before cooling again to 25 °C (10 °C/min). This alternating heating and cooling was repeated, with T_s being lowered at 5 °C intervals, with respect to the previous step, from 135 to 60 °C for the homopolymers and from 125 to 60 °C for the copolymers. Final melting endotherms were obtained by the polymer being heated to 170 °C (10 °C/min).

^{13}C NMR spectra were recorded on a Bruker Avance 400 spectrometer. The acquisition time was 2 s, the delay time between pulses was 7 s, and the number of scans was 6000. The characterizations were carried out as reported earlier.[23]

RESULTS AND DISCUSSION

Polymerization Activities

To study the effects of different methyl-substitution patterns on the Cp ligand, ethene was homopolymerized and copolymerized with 1-hexene under the same conditions. Figure 1 shows the activities of ethene/1-hexene copolymerizations for all the catalysts described previously. The activity profiles of the copolymerizations differ from those obtained in homopolymerization. An example is shown for $R_n = Me_4$ in Figure 2. During homopolymerization, there is a maximum in ac-

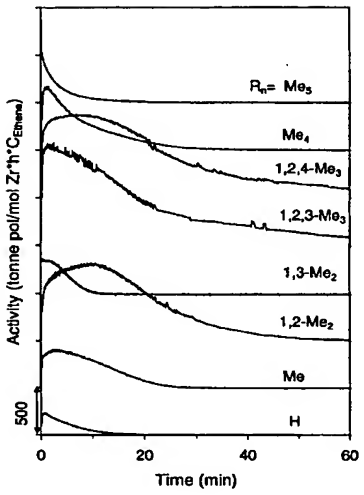

Figure 1. Polymerization rate as a function of the reaction time for ethene/1-hexene copolymers synthesized with $(R_nC_5H_{5-n})_2ZrCl_2$/MAO catalysts. Activity curves are displaced in steps of 500 along the vertical axis. T = 80 °C; P_{ethene} = 2 bar; [H] = 0.4 M; [Al]/[Zr] = 3000.

tivity only a few seconds after the catalyst addition followed by a strong deactivation for 5–10 min. The maximum activity in copolymerization is reached after 2–10 min, and the deactivation is much slower than in the homopolymerization. Table I shows that the substitution pattern of the ligand has no particular effect on the catalytic activity of homopolymerization, although somewhat lower activities are observed with R_n = Me_4 and R_n = Me_5. A positive comonomer effect after the addition of 1-hexene was observed for all catalysts except for R_n = H and R_n = 1,3-Me_2. For R_n = Me_5, there is no significant change in activity after 1-hexene addition, but in this case the comonomer incorporation is very low (0.3%), and the shape of the copolymerization activity profile resembles that of a typical homopolymerization. Several studies on the effect of comonomer addition have been reported,[2,24–26] and explanations of the enhanced activity are given in terms of activation of dormant sites, increased insertion rate of ethene due to an electronic influence of the comonomer,[27] and increased ethene solubility and, therefore, reduced diffusion limitation.[2] All the copolymers, except those synthesized with R_n = Me_5, were dissolved in the toluene when the reactor was opened. This might indicate that reduced diffusion limitation in copolymerization could explain the positive comonomer effect obtained with most of the catalysts. Some of the runs were reproduced, and there is good reproducibility with respect to the melting point and molecular weight, whereas the polymerization activity is in general less reproducible. However, in a new series of experiments, the unexpected results for R_n = 1,3-Me_2 were checked, and it was verified that this catalyst shows a negative comonomer effect. One explanation for the high variability in polymerization kinetics is given by Huang and Rempel.[28] They proposed that residual oxygen reacts with residual trimethylaluminum (TMA) present in the MAO cocatalyst. Small fluctuations in the oxygen concentration can translate into changes in the concentration and chemistry of the MAO solution, which may give rise to the high variance in kinetic measurements involving metallocenes.[29] This has to be considered in comparisons of the activities obtained with different catalysts.

Comonomer Response

The 1-hexene content of the copolymers lies between 0.3 and 5.5 mol % and is in the range quoted for similar systems.[24,30] As displayed in Figure 3, with an increasing number of methyl substituents on the Cp ligand, there is a tendency toward lower 1-hexene incorporation in the copolymer. For the dimethyl-substituted and trimethyl-substituted catalysts, there are two possible substitution patterns, and the R_n = 1,3-Me_2 and R_n = 1,2,4-Me_3 catalysts show a higher degree of 1-hexene incorporation than R_n = 1,2-Me_2 and R_n

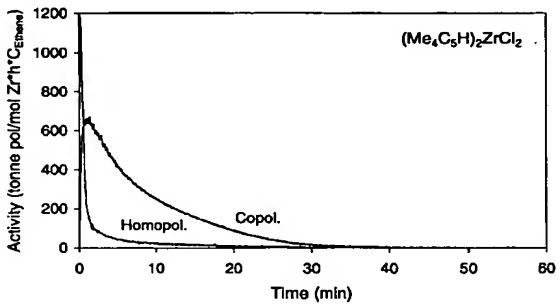

Figure 2. Polymerization rate as a function of the reaction time for the homopolymerization of ethene and the copolymerization of ethene/1-hexene with $(Me_4C_5H)_2ZrCl_2$/MAO. T = 80 °C; P_{ethene} = 2 bar; [Zr] = 1.2 μM; [Al]/[Zr] = 3000; [H] = 0.4 M for the copolymerization.

Table I. Experimentally Obtained Activity and Polymer Characteristics from the Homopolymerization and Copolymerization of Ethene and 1-Hexene Synthesized with $(R_nC_5H_{5-n})_2ZrCl_2$/MAO Catalysts (R_n = H; Me; 1,2-Me_2; 1,3-Me_2; 1,2,3-Me_3; 1,2,4-Me_3; Me_4; or Me_5)

Run	Substituent (R_n)	[H][a]	[H] in Polymer (mol %)[b]	*trans*-Vinylene/ Vinyl/Vinylidene[c]	Activity[d]	T_m (°C)[e]	M_n (g/mol) · 10^{-3} [f]	M_n (g/mol) · 10^{-3} [g]	M_w (g/mol) · 10^{-3} [g]	PD[g]
26	H	0			71	135.2		49.4	102	2.0
41		0		0.022/0.212/0	108	134.9	111	84.1	164	1.9
27		0.40			29	110.5		14.3	23.9	1.7
28		0.40			11	112.3		13.3	22.1	1.7
42		0.40	2.7	0.048/0.170/0.719	22	112.4	15.7	11.0	23.6	2.1
58	Me	0		0.026/0.162/0	47	136.2	78.0	72.4	179	2.5
60		0.40	2.5	0.033/0.153/0.417	88	115.3	24.4	25.5	48.9	1.9
51	1,2-Me_2	0		0.015/0.036/0	91	138.5	283	113	246	2.2
54		0.40			5.4	118.0		47.7	118	2.5
56		0.40	1.8	0.033/0.073/0.155	314	118.0	55.7	57.2	95.9	1.7
48	1,3-Me_2	0		0.017/0.054/0	59	140.3	216	96.5	223	2.3
50		0.40	4.0	0.028/0.081/0.225	29	111.0	45.3	34.1	107	3.1
32	1,2,3-Me_3	0		0.026/0.029/0	49	138.1	262	109	243	2.2
33		0.40			202	121.2		84.0	140	1.7
34		0.40	1.7	0.030/0.036/0.105	334	120.7	84.6	65.2	105	1.6
61		0.40			10	120.0		96.8	170	1.8
23	1,2,4-Me_3	0		0.028/0.057/0	87	138.2	182	142	308	2.2
24		0.40	5.5	0.022/0.049/0.226	361	111.0	52.4	51.6	79.5	1.5
62		0.40			133	110.5		56.2	87.8	1.6
19	Me_4	0		0.012/0.059/0	22	137.5	202	98.0	244	2.5
36		0.40			88	119.4		68.5	117	1.7
38		0.40	1.4	0.013/0.013/0.034	99	118.7	239[h]	73.0	119	1.6
29	Me_5	0		0.081/0.080/0	26	138.0	87.5	48.3	108	2.2
30		0.40	0.3	0.104/0.071/0.015	31	130.0	74.2	47.3	84.2	1.8

T = 80 °C; P_{ethene} = 2 bar; [Al]/[Zr] = 3000; solvent-toluene; [E] = 0.143 mol/L; [Zr] = 1.2 μM (except for run 48, 50, 51, 54, where [Zr] = 0.6 μM).

[a] Initial concentration of 1-hexene in the reactor (mol/L).
[b] Determined by ^{13}C NMR.
[c] Determined by FTIR per 1000 C in the polymer backbone.
[d] Tonne PE/(mol Zr · h · C_{ethene}).
[e] Determined by DSC.
[f] Determined by FTIR.
[g] Determined by GPC.
[h] Uncertain value (irregular IR spectrum).

= 1,2,3-Me_3. There is a twofold increase in 1-hexene incorporation by the position of the methyl substituents being changed. Most amazing is that R_n = 1,3-Me_2 incorporates more 1-hexene than R_n = Me and that the R_n = 1,2,4-Me_3-based polymer contains three times as much 1-hexene as the one based on R_n = 1,2-Me_2. As expected, the pentamethyl-substituted catalyst shows the lowest comonomer response. The variation in the comonomer incorporation with the methyl-substitution pattern is, at least qualitatively, in agreement with the results of a theoretical study conducted in parallel with the experiments. Using density functional theory, we modeled the insertion of ethene and an α-olefin into cationic $(R_nC_5H_{5-n})_2ZrC_4H_9^+$. On the basis of numerous earlier investigations of similar systems,[12,31,32] it is assumed that a typical insertion reaction goes through a four-center α-agostic transition state, characterized by a distance of about 2.20 Å between the C_2 atom of the (co)monomer and the C_α atom of the growing polymer chain (i.e., the new C—C bond formed during insertion). A linear butyl is selected to represent the growing chain under the assumption that the last inserted monomer was ethene. Furthermore, a computationally less demanding 1-butene is used to model the insertion of 1-hexene, and it is assumed that the comonomer is predominantly 1,2 inserted (see the following discussion). In Figure 4(a), optimized (approximate) transition states are shown for the insertion of 1-butene into the disubstituted and

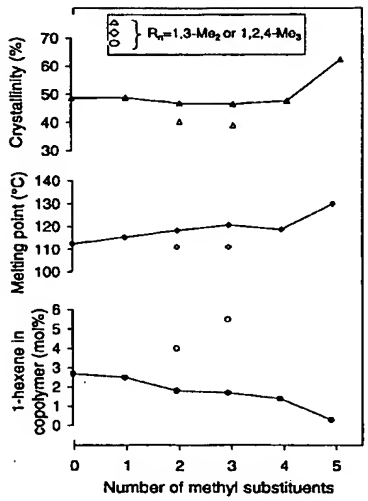

Figure 3. Incorporation of the 1-hexene (mol %), melting point (°C), and crystallinity (%) of ethene/1-hexene copolymers as a function of the number of methyl substituents on the Cp ligand. Catalysts = $(R_nC_5H_{5-n})_2ZrCl_2$/MAO (R_n = H, Me, 1,2-Me_2, 1,3-Me_2, 1,2,3-Me_3, 1,2,4-Me_3, Me_4, or Me_5); T = 80 °C; P_{ethene} = 2 bar; [Zr] = 1.2 μM; [Al]/[Zr] = 3000; [H] = 0.4 M.

trisubstituted catalysts. With a split methyl-substitution pattern, all the substituents are pointing away from the comonomer coordination site. However, for R_n = 1,2-Me_2 and, in particular, for R_n = 1,2,3-Me_3, the energetically preferred configurations have one or two methyl substituents pointing into the comonomer coordination site, thereby increasing the steric hindrance of comonomer insertion. In this manner, it can also be rationalized that adding one more split methyl substituent to R_n = 1,2-Me_2 increases the comonomer incorporation as space then is created at the insertion point. The trends can be quantified in terms of energetic and geometric parameters, as shown in Figure 4(b). In the lower curve, we plotted the difference in the binding energy in the transition states of 1-butene and ethene insertion. The middle curve is a plot of the sum (absolute values) of the two dihedral angles Zr–C_1–C_2–C_3 and Zr–C_1–C_α–C_β [see Fig. 4 (a)] evaluated in the transition state of 1-butene insertion. These dihedrals are expected to give a measure of the steric repulsion between an $R_nC_5H_{5-n}$ ligand and, respectively, the ethyl group of 1-butene and the growing polymer chain. Finally, in the upper curve we plotted the total hydrogen–hydrogen overlapping volume, also evaluated in the transition state of 1-butene insertion. All three parameters show the expected trend, with increasing values after the addition of methyl substituents. Moreover, the lower values for the split methyl-substituted catalysts are in agreement with a higher degree of comonomer incorporation. However, the calculations cannot explain why these catalysts incorporate more comonomer than R_n = Me and R_n = H.

The dyad sequence distributions were assigned according to Randall and Hsieh[33] and were used for the calculation of the monomer reactivity ratios (Table II) and 1-hexene incorporation. It can be concluded that the 1-hexene incorporation in the polymer decreases in the following order: R_n = 1,2,4-Me_3 > 1,3-Me_2 > H > Me > 1,2-Me_2 > 1,2,3-Me_3 > Me_4 > Me_5. The numerical value of the product $r_E \cdot r_H$ is higher than 1 for all catalysts, indicating that there is a tendency for the two monomers to incorporate in separate blocks. As might be expected, a decrease in r_E from 1012 to 64 is observed by the substitution pattern being changed from R_n = Me_5 to R_n = 1,2,4-Me_3 in accordance with the amount of 1-hexene incorpo-

Table II. ^{13}C NMR Analysis of Ethene/1-Hexene Copolymers Synthesized with $(R_nC_5H_{5-n})_2ZrCl_2$/MAO Catalysts (R_n = H; Me; 1,2-Me_2; 1,3-Me_2; 1,2,3-Me_3; 1,2,4-Me_3; Me_4; or Me_5)

Run	Substituent (R_n)	[EH]	[HH]	[EE]	[E]	[H]	r_E	r_H	$r_E \cdot r_H$
42	H	4.7	0.3	95.0	97.3	2.7	114	0.052	5.9
60	Me	4.0	0.5	95.5	97.5	2.5	132	0.090	12
56	1,2-Me_2	2.6	0.3	97.1	98.2	1.8	205	0.083	17
50	1,3-Me_2	6.8	0.6	92.6	96.0	4.0	75	0.058	4.4
34	1,2,3-Me_3	3.3	0.1	96.6	98.3	1.7	161	0.016	2.6
24	1,2,4-Me_3	7.9	1.5	90.6	94.5	5.5	64	0.14	9.0
38	Me_4	2.1	0.3	97.6	98.6	1.4	253	0.11	28
30	Me_5	0.55	0.04	99.41	99.7	0.3	1012	0.055	56

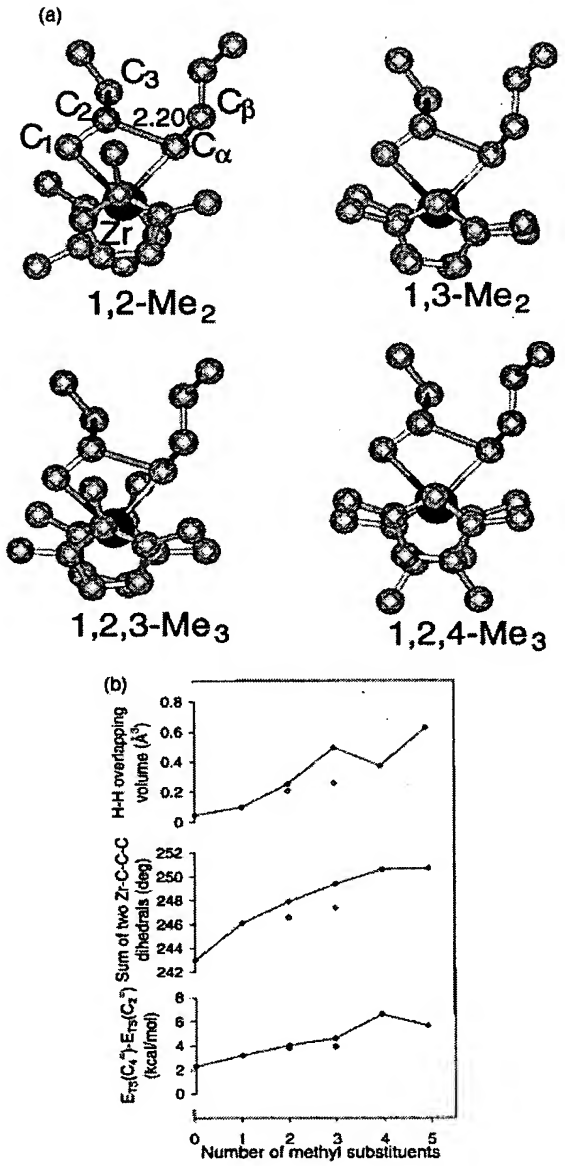

Figure 4. (a) Approximate α-agostic transition states of 1-butene insertion into the disubstituted and trisubstituted catalysts, optimized with density functional theory. (b) Theoretical measures of comonomer incorporation as derived from density functional theory optimized transition states of insertion and plotted as a function of the number of methyl substituents on the Cp ligands. Lower curve: difference in the binding energy between 1-butene and ethene insertion (kcal/mol). Middle curve: sum (absolute values) of the two dihedral angles Zr–C_1–C_2–C_3 and Zr–C_1–C_α–C_β in the transition state of 1-butene insertion. Upper curve: total overlapping volume (Å^3) between pairs of hydrogen atoms in the transition state of 1-butene insertion. An atomic radius of 1.1 Å was used for hydrogen. The open symbols represent R_n = 1,3-Me_2 and 1,2,4-Me_3.

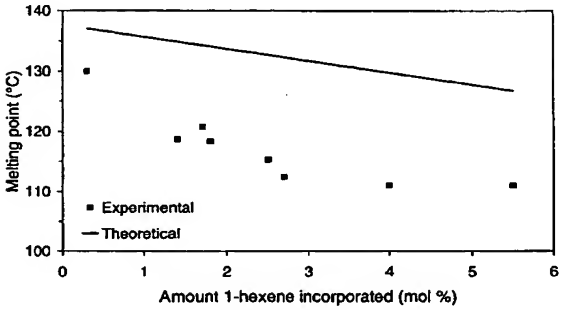

Figure 5. Melting point of the ethene/1-hexene copolymers as a function of the amount of 1-hexene incorporated. Catalysts = $(R_nC_5H_{5-n})_2ZrCl_2$/MAO (R_n = H, Me, 1,2-Me_2, 1,3-Me_2, 1,2,3-Me_3, 1,2,4-Me_3, Me_4, or Me_5). T = 80 °C; P_{ethene} = 2 bar; [Zr] = 1.2 μM; [Al]/[Zr] = 3000; [H] = 0.4 M. The solid line represents the theoretical prediction (see the text).

rated. A dramatic increase in the concentration of [HH] dyads from 0.1 to 1.5% is found by the substitution pattern being changed from R_n = 1,2,3-Me_3 to R_n = 1,2,4-Me_3.

Crystallization and Melting

There is a significant depression of the melting point (T_m) of the copolymers compared with their homopolymer analogues, as shown in Table I. The reduction in T_m varies between 9 °C (R_n = Me_5) and 29 °C (R_n = 1,3-Me_2). As can be seen from Figure 3, the trend is that increased methyl substitution gives higher melting points, again with the exceptions of R_n = 1,3-Me_2 and R_n = 1,2,4-Me_3, which display low melting points in accordance with their high comonomer content. The correlation between the melting point of the copolymers and the amount of 1-hexene incorporated is shown in Figure 5. The Flory equation for copolymerization[34] is plotted in the same figure:

$$\frac{1}{T_m} - \frac{1}{T_m^0} = -\frac{R}{\Delta H_u} \cdot \ln(X_E)$$

where ΔH_u is the heat of fusion per polymer repeating unit, X_E is the molar fraction of the crys-

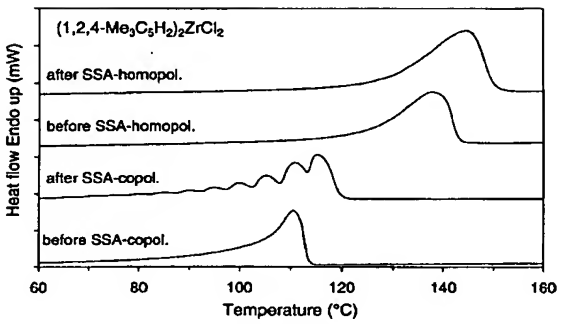

Figure 6. Melting endotherms of the ethene homopolymer and the copolymer of ethene/1-hexene before and after the application of SSA. Catalyst = (1,2,4-$Me_3C_5H_2)_2ZrCl_2$/MAO.

tallizing unit (ethene), T_m^0 is the melting temperature of the homopolymer, and T_m is the melting temperature of the copolymer. The average experimental values from the homopolymerization of ethene are used for both ΔH_u and T_m^0. The experimentally observed melting points for the copolymers lie between 7 and 20 °C below the theoretical line, and this is qualitatively in accordance with what is reported elsewhere.[24,30,35] The theoretical calculation is based on a truly random copolymer and requires that total equilibrium prevails throughout the system. This is very difficult to achieve even under the most stringent crystallization conditions.[36] All polymers were fractionated by SSA, a DSC technique described by Müller et al.[22] This procedure based on successive annealing allows melt/melt and melt/solid segregation to occur during thermal cycles that promote self-nucleation, crystallization, and annealing processes. The technique makes separation by short chain branching possible and, as a result, the observation of structural heterogeneity. A comparison of the melting endotherm of the copolymer synthesized with the R_n = 1,2,4-Me_3 catalyst before and after the fractionation procedure is shown in Figure 6. The melting curve of the former shows a single peak and a narrow distribution of lamellar thicknesses, whereas after the application of SSA, a separation of different molecular species has taken place because of the difference in their lamellar thickness.[37] The final melting endotherms of all the copolymers studied by the SSA technique are compared in Figure 7. The copolymers show different peaks and peak heights depending on the amount of 1-hexene incorporated. The values of the highest peak for each catalyst are shifted toward lower temperatures with higher comonomer incorporation. The catalysts that incorporated the highest amount of 1-hexene (R_n = 1,2,4-Me_3, R_n = 1,3-Me_2, and R_n = H) have rather equal sizes of the different peaks compared with the catalysts with lower incorporation of comonomer. This is in accordance with what was observed by Starck et al.[37] for ethene/1-hexene copolymers produced by metallocenes. They claimed that this indicates a more homogeneous comonomer distribution of the former. In their study, they applied a segregation fractionation technique by DSC where the sample was annealed in steps at successively decreasing temperatures without cooling between the steps. In Figure 6, we also included the melting endotherms of the homopolymers synthesized with R_n = 1,2,4-Me_3 before and after applying SSA. There is no fractionation for the homopolymer, but the peak value is 6 °C higher compared with the ordinary DSC run showing a more well-defined crystallization.

The crystallinity of the copolymers was calculated according to the literature[38] and plotted as a function of the number of methyl substituents in Figure 3 with the heat of fusion of polyethene assumed to be 269.9 J/g. As expected, a higher degree of crystallization was found for R_n = Me_5, and the low values for the split methyl-substituted catalysts are consistent with the high degree of comonomer incorporation.

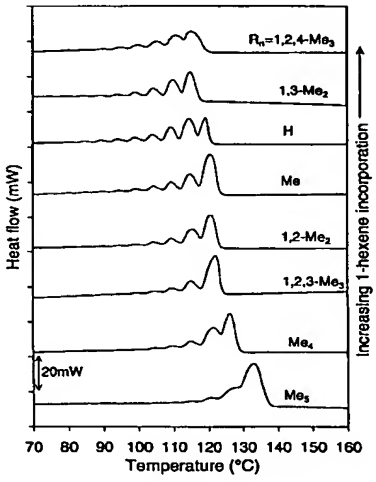

Figure 7. Melting endotherms of the copolymers of ethene/1-hexene after the application of SSA. Catalysts = ($R_nC_5H_{5-n})_2ZrCl_2$/MAO (R_n = H, Me, 1,2-Me_2, 1,3-Me_2, 1,2,3-Me_3, 1,2,4-Me_3, Me_4, or Me_5).

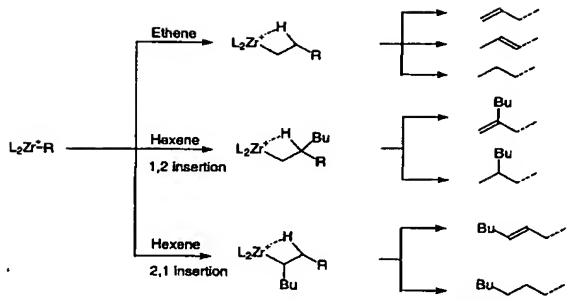

Scheme 2. Different termination reactions during ethene/1-hexene copolymerization. With ethene as the last inserted monomer, followed by β-hydrogen elimination or β-hydrogen transfer to coordinated monomer, there is vinyl unsaturation. With 1-hexene as the last inserted monomer, these termination mechanisms result in a vinylidene unsaturation after a 1,2 insertion and a *trans*-vinylene unsaturation after a 2,1 insertion. After ethene insertion, an isomerization reaction followed by chain termination produces *trans*-vinylene unsaturations. Chain transfer to TMA is possible, both after ethene and 1-hexene insertion, and results in saturated end groups.

Molecular Weight and Chain Termination

Polymer unsaturations are determined by FTIR spectroscopy of the homopolymers of ethene and the copolymers of ethene and 1-hexene. The homopolymers contain vinyl and *trans*-vinylene unsaturations, whereas the copolymers also contain vinylidene. The most relevant termination reactions during homopolymerization and copolymerization are shown in Scheme 2. Vinyl unsaturations are produced by β-hydrogen elimination or β-hydrogen transfer to monomer with ethene as the last inserted monomer. If the last monomer is 1-hexene, these termination mechanisms will result in a vinylidene unsaturation after a 1,2 insertion and a *trans*-vinylene unsaturation after a 2,1 insertion. The observed *trans*-vinylene unsaturations resulting from the homopolymerization of ethene[12] can be explained in terms of an isomerization reaction followed by termination. For some catalysts, chain transfer to TMA is an important termination mechanism.[12,39] After the polymer has been exposed to water, this results in saturated end groups and is usually reflected in significantly higher number-average molecular weight (M_n) values as determined by FTIR, in comparison with GPC measurements. In Figure 8, the concentrations of the unsaturations for both the homopolymers and the copolymers are plotted as a function of the number of methyl substituents on the Cp ligand. The unsaturations and, therefore, the termination mechanisms are dependent on the substitution pattern of the catalyst. However, there are, as a first approximation, rather small differences between the vinyl and *trans*-vinylene unsaturations of the homopolymers and copolymers. Therefore, as might be expected, termination after an ethene insertion is unaffected by the presence of the comonomer. Furthermore, it is self-evident that vinylidene, from termination after the 1,2 insertion of 1-hexene in the copolymers, dominates for most of the catalysts, with a noticeable exception as the full substitution of the Cp ligands is approached. We also see that the most open ligands, R_n = H and R_n = Me, allow easier overall termination for both the homopolymers and copolymers, as clearly verified by the molecular weights (shown later in Fig. 11). That Cp* also enhances termination obviously must be due to other effects. Furthermore, because the concentration of *trans*-vinylene unsaturations in the homopolymers is lower than that of vinyl for all catalysts except R_n = Me_5, the tendency of chain-end isomerization is low except for the latter catalyst. This is in agreement with earlier studies in which a higher amount of *trans*-vinylene unsaturation was found for R_n = Me_5 than for R_n = H.[12] These findings could be rationalized in terms of an easier chain-end isomerization, relative to termination, for R_n = Me_5 than for R_n = H. The *trans*-vinylene concentration is consistently somewhat higher in the copolymers than in the corresponding homopolymers. This may be attributed to some chain ter-

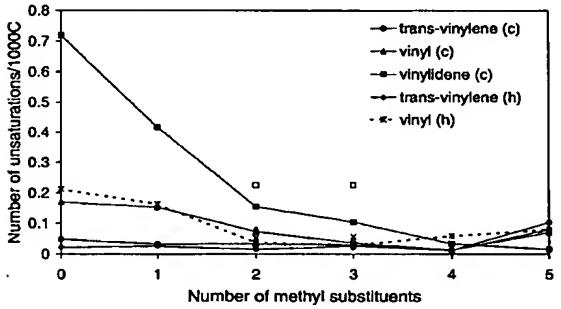

Figure 8. Number of vinyl, vinylidene, and *trans*-vinylene unsaturations per 1000 C in the polymer backbone as a function of the number of methyl substituents on the Cp ligand. The open symbols and the multiplication symbol represent R_n = 1,3-Me_2 and 1,2,4-Me_3. h = homopolymer; c = copolymer.

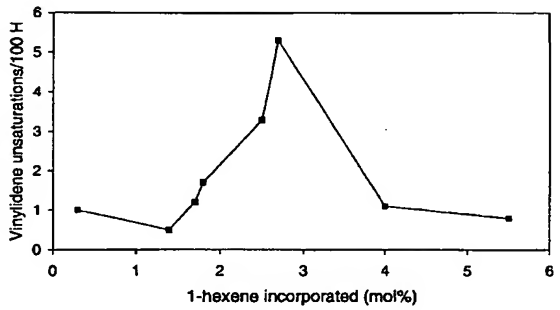

Figure 9. Number of vinylidene unsaturations per 100 inserted comonomers as a function of the comonomer incorporation.

mination following a 2,1 insertion of 1-hexene. However, the difference is small, most likely suggesting that 2,1 insertion is not significant or possibly that chain termination after 2,1 insertion is suppressed. In Figure 9, we plotted the number of vinylidene unsaturations per 100 inserted comonomers as a function of the comonomer incorporation. This figure shows that there is a tendency of more frequent termination after each hexene insertion with increasing comonomer incorporation up to about 3%. The two catalysts containing split methyl substitutions behave differently. Most likely, these effects are steric, as seen from a plot of the same data as a function of the number of methyl substituents (Fig. 10). We find that not only does the addition of successively adjacent methyls to the R_n = H catalyst decrease the comonomer-induced termination as a whole but the termination probability per 1-hexene incorporated also is reduced. Again, we notice that

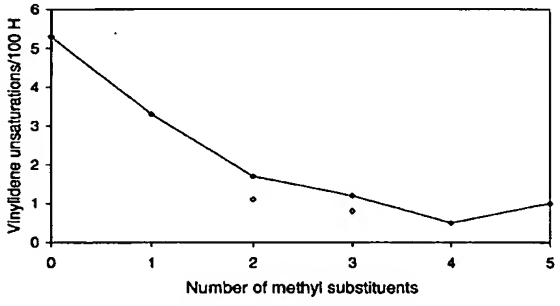

Figure 10. Number of vinylidene unsaturations per 100 inserted comonomers as a function of the number of methyl substituents. The open symbols represent R_n = 1,3-Me_2 and 1,2,4-Me_3.

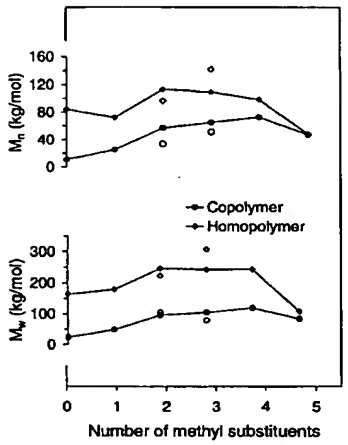

Figure 11. M_n and M_w as a function of the number of methyl substituents on the Cp ligand. The open symbols represent R_n = 1,3-Me_2 and 1,2,4-Me_3. T = 80 °C; P_{ethene} = 2 bar; [Zr] = 1.2 μM; [Al]/[Zr] = 3000; [H] = 0.4 M for the copolymerization.

for R_n = 1,3-Me_2 and R_n = 1,2,4-Me_3, termination after the 1,2 insertion of 1-hexene is atypical and more difficult than for R_n = 1,2-Me_2 and R_n = 1,2,3-Me_3. Note the reverse order of these catalysts in Figures 8 and 10. Still, the main conclusion to be drawn from these results is that the termination probability per inserted comonomer is highest for the less substituted catalysts, R_n = H and R_n = Me. As could be expected, this suggests that less methyl substitution results in an easier rotation of the growing polymer chain, from a γ-agostic configuration to a β-agostic configuration, and an easier transfer of the β-hydrogen. Figure 10 shows that, depending on the methyl-substitution pattern, between 0.5 and 5.3% of the inserted 1-hexene results in chain termination. Analogously, one may calculate the number of vinyl and *trans*-vinylene unsaturations per 100 inserted ethene monomers, both for the homopolymers and copolymers. These numbers lie in the range 0.002–0.035, showing that termination after the 1,2 insertion of 1-hexene is roughly 100 times more likely than after insertion of ethene.

The substitution pattern also influences the molar masses of the polymers, as shown in Figure 11. Most remarkable is the high molecular weight for the R_n = 1,2,4-Me_3 homopolymer and also for the copolymer in view of its high 1-hexene content. A comparison of M_n from FTIR and GPC (Table I) indicates a small difference for the ho-

mopolymer of R_n = 1,2,4-Me_3 and probably a reduced transfer to the cocatalyst. It is gratifying that M_n(FTIR) > M_n(GPC) for the homopolymers and M_n(FTIR) ≈ M_n(GPC) for most of the copolymers where other termination reactions become dominant. In all cases, the molar masses of the copolymers are lower than those of the ethene homopolymers, and this is in accordance with what is observed by others.[2] Reasons for this may be the lower rate of comonomer insertion, enhanced chain transfer to comonomer, and more facile β-hydrogen elimination from a 1,2 inserted comonomer due to the tertiary nature of its β-hydrogen atom.[11] The data definitely support the latter explanation, as vinylidene is the dominating end group for the copolymers.[40] The observed molecular weight distributions are narrow, with M_w/M_n (weight-average molecular weight/number-average molecular weight) between 2.0 and 2.5 for the homopolymers and between 1.5 and 3.1 for the copolymers.[41] For all the catalysts except R_n = 1,3-Me_2, the polydispersity is lower for the copolymers than for the respective homopolymers. This might be due to a more homogeneous termination during copolymerization.

CONCLUSIONS

Ethene homopolymerization and copolymerization with 1-hexene for the series of catalysts $(R_nC_5H_{5-n})_2ZrCl_2$, with R_n = H, Me, 1,2-Me_2, 1,2,3-Me_3, Me_4, or Me_5, are characterized by the following:

- With an increasing number of methyl substituents on the Cp ligand, there is a tendency toward lower 1-hexene incorporation and, consequently, higher melting points of the copolymers.
- The addition of 1-hexene causes an increase in the polymerization activity for all these catalysts except R_n = H.
- End-group analysis shows that termination after an ethene insertion is unaffected by the presence of the comonomer.
- The most open ligands, R_n = H and R_n = Me, allow easier overall termination for both homopolymerization and copolymerization and, consequently, lower molecular weights.
- There is a tendency of more frequent termination after each hexene insertion with increasing comonomer incorporation.
- With an increasing number of methyl substituents on the Cp ligand, there is a decrease in the comonomer induced termination as a whole and termination probability per 1-hexene incorporated. From a mechanistic point of view, this suggests a more hindered rotation from a γ-agostic conformation to a β-agostic conformation and also a higher termination barrier with increased methyl substitution.

In addition, some special effects for R_n = 1,3-Me_2 and R_n = 1,2,4-Me_3 comprise the following:

- They show a higher 1-hexene incorporation than their disubstituted and trisubstituted analogues and an even higher incorporation than R_n = H and R_n = Me.
- Termination after 1,2 insertion of 1-hexene is more difficult than for R_n = 1,2-Me_2 and R_n = 1,2,3-Me_3.
- The catalyst with R_n = 1,2,4-Me_3 produces a copolymer with an unusual combination of high comonomer incorporation and relatively high molecular weight.

This work has received support from the Research Council of Norway under the Reactor Technology in the Petrochemistry and Polymer Industry (REPP) program and the Programme for Supercomputing. Borealis is acknowledged for financial support.

REFERENCES AND NOTES

1. Brintzinger, H. H.; Fischer, D.; Mülhaupt, R.; Rieger, B.; Waymouth, R. M. Angew Chem Int Ed Engl 1995, 34, 1143–1170.
2. Koivumaki, J.; Seppälä, J. V. Macromolecules 1993, 26, 5535–5538.
3. Tsutsui, T.; Kashiwa, N. Polym Commun 1988, 29, 180–183.
4. Kaminsky, W. Stud Surf Sci Catal 1986, 25, 293–304.
5. Quijada, R.; Dupont, J.; Lacerda Miranda, M. S.; Scipioni, R. B.; Galland, G. B. Macromol Chem Phys 1995, 196, 3991–4000.
6. Suhm, J.; Schneider, M. J.; Mülhaupt, R. J Mol Catal A: Chem 1998, 128, 215–227.
7. Kaminsky, W. Macromol Chem Phys 1996, 197, 3907–3945.
8. Möhring, P. C.; Coville, N. J. J Mol Catal A: Chem 1995, 96, 181–195.
9. Schneider, M. J.; Suhm, J.; Mülhaupt, R.; Prosenc, M.-H.; Brintzinger, H. H. Macromolecules 1997, 30, 3164–3168.

10. Yoon, J.; Lee, D.-H. P. E.-S.; Lee, I.-M.; Park, D.-K.; Jung, S.-O. J Appl Polym Sci 2000, 75, 928–937.
11. Lehmus, P.; Harkki, O.; Leino, R.; Luttikhedde, H.; Nasman, J.; Seppälä, J. Macromol Chem Phys 1998, 199, 1965–1972.
12. Thorshaug, K.; Støvneng, J. A.; Rytter, E.; Ystenes, M. Macromolecules 1998, 31, 7149–7165.
13. Kokko, E.; Malmberg, A.; Lehmus, P.; Löfgren, B.; Seppälä, J. V. J Polym Sci Part A: Polym Chem 2000, 38, 376–388.
14. ADF 2.3, Scientific Computing and Modelling, Chemistry Department, Vrije Universiteit, Amsterdam, The Netherlands, 1993. We used a double-ζ STO basis set for C and H and a triple-ζ STO basis set for Zr. The 1s to 3d orbitals on Zr and the 1s orbital on C were treated within the frozen core approximation. Geometries were optimized within the local density approximation,[15] and gradient corrections to the energy were based on the functionals proposed by Becke[16] and Perdew and Wang.[17]
15. Vosko, S. H.; Wilk, L.; Nusair, M. Can J Phys 1980, 58, 1200–1211.
16. Becke, A. D. Phys Rev A: At Mol Opt Phys 1988, 38, 3090–3100.
17. Perdew, J. P.; Wang, Y. Phys Rev B: Condens Matter 1992, 45, 13244–13249.
18. Blom, R.; Follestad, A.; Noel, O. J Mol Catal 1994, 91, 237–249.
19. Quijada, R.; Rojas, R.; Mauler, R. S.; Galland, G. B.; Scipioni, R. B. J Appl Polym Sci 1997, 64, 2567–2574.
20. Thorshaug, K.; Støvneng, J. A.; Rytter, E. Macromolecules, submitted for publication, 1999.
21. Thorshaug, K.; Rytter, E.; Ystenes, M. Macromol Rapid Commun 1997, 18, 715–722.
22. Müller, A.; Hernandez, Z.; Arnal, M.; Sanchez, J. Polym Bull 1997, 39, 465–472.
23. Wester, T.; Johnsen, H.; Kittilsen, P.; Rytter, E. Macromol Chem Phys 1998, 199, 1989–2004.
24. Chien, J. C.; Nozaki, T. J Polym Sci Part A: Polym Chem 1993, 31, 227–237.
25. Olabisi, O.; Atiqullah, M.; Kaminsky, W. J Macromol Sci Rev Macromol Chem Phys 1997, 37, 519–554.
26. Herfert, N.; Montag, P.; Fink, G. Makromol Chem 1993, 194, 3167–3182.
27. Kaminsky, W.; Arndt, M. Adv Polym Sci 1997, 127, 143–187.
28. Huang, J.; Rempel, G. Polym React Eng 1997, 5, 125–139.
29. D'Agnillo, L.; Soares, J. B. P.; Penlidis, A. J Polym Sci Part A: Polym Chem 1998, 36, 831–840.
30. Koivumäki, J.; Lahti, M.; Seppälä, J. V. Angew Makromol Chem 1994, 221, 117–125.
31. Fan, L.; Harrison, D.; Woo, T. K.; Ziegler, T. Organometallics 1995, 14, 2018–2026.
32. Busico, V. C. R. J Am Chem Soc 1994, 116, 9329–9330.
33. Randall, J. C.; Hsieh, E. T. In NMR and Macromolecules: Sequence, Dynamic, and Domain Structure; Randall, Jr., J. C., Ed.; ACS Symposium Series 247; American Chemical Society: Washington, DC, 1984; pp 131–151.
34. Billmeyer, F. W. Textbook of Polymer Science; Wiley: New York, 1984; p 336.
35. Rudolph, S.; Giesemann, J.; Kressler, J.; Menke, T.; Menge, H.; Arends, P. J Appl Polym Sci 1999, 74, 439–447.
36. Alamo, R.; Mandelkern, L. Thermochim Acta 1994, 238, 155–201.
37. Starck, P.; Lehmus, P.; Seppälä, J. Polym Eng Sci 1999, 39, 1444–1455.
38. Soga, K.; Uozumi, T.; Park, J. R. Makromol Chem 1990, 191, 2853–2864.
39. Ystenes, M.; Eilertsen, J. L.; Liu, J.; Ott, M.; Rytter, E.; Støvneng, J. A. J Polym Sci Part A: Polym Chem, in press.
40. A β-agostic configuration after the 1,2 insertion of a comonomer that is more reactive than a configuration after the insertion of ethene is also consistent with the observed positive comonomer effect.
41. The observed molar mass distributions are generally narrower than expected for single-site catalysts (M_w/M_n should not be smaller than 2.0). This is probably because two GPC columns are insufficient to give a good separation of the polymer in this case. As a part of another study, some of the samples were analyzed in another GPC instrument equipped with three columns. Those results show a somewhat higher polydispersity for the polymers. The M_w values are higher than those obtained in our study, whereas the M_n values are the same. It seems that the shift in M_w is almost equal for all the polymers, so the trends will remain the same.